Archive of Applied Mechanics 68 (1998) 433–444 © Springer-Verlag 1998

Thermoelectroelastic Green's function and its application for bimaterial of piezoelectric materials

Qing-Hua Qin, Yiu-Wing Mai

Summary For a two-dimensional piezoelectric plate, the thermoelectroelastic Green's functions for bimaterials subjected to a temperature discontinuity are presented by way of Stroh formalism. The study shows that the thermoelectroelastic Green's functions for bimaterials are composed of a particular solution and a corrective solution. All the solutions have their singularities, located at the point applied by the dislocation, as well as some image singularities, located at both the lower and the upper half-plane. Using the proposed thermoelectroelastic Green's functions, the problem of a crack of arbitrary orientation near a bimaterial interface between dissimilar thermopiezoelectric material is analysed, and a system of singular integral equations for the unknown temperature discontinuity, defined on the crack faces, is obtained. The stress and electric displacement (SED) intensity factors and strain energy density factor can be, then, evaluated by a numerical solution at the singular integral equations. As a consequence, the direction of crack growth can be estimated by way of strain energy density theory. Numerical results for the fracture angle are obtained to illustrate the application of the proposed formulation.

Key words piezoelectric plate, Green function, bimaterial, crack, interface, thermal stress

1 Introduction

In engineering practice, most structures contain internal interfaces. When a heat flow in a structure is disturbed by some defects, such as holes or cracks, the local temperature gradient around the defects is increased, and the temperature is often discontinuous across the defects. Thermal disturbances of this type may produce material failure. Therefore, the thermal analysis for such structures is very important in engineering. A number of studies dealing with flaw-induced thermal stresses in infinite regions has been done [1–3]. Applying the equations for the distribution of thermal stresses in an anisotropic elastic half-space, [4], a solution for the two-dimensional Griffith crack obstructing a uniform heat flow in a general anisotropic medium as given in [5]. Using the techniques of Fourier transforms and multiple integration, the penny-shaped crack embedded in a transversely isotropic or orthotropic material was studied in [6]. Based on the Stroh's formalism and complex conformal mapping, thermal stresses for an anisotropic elastic plate with an elliptic hole subjected to uniform heat flow in x_2-direction were obtained in [7]. The above authors used complex-variable methods or Fourier transforms to represent the stress and displacement fields. An alternative method, which has been extensively used in thermoelastic problems, is to represent the elastic fields in terms of Green's function [8]. It is well known that the Green's function method has some important advantages over the above-mentioned methods, such as transform methods. First, we note that the solution is expressed in terms of physical variables so that it is easier to determine at intermediate stages whether the solution is physically reasonable [9]. In particular, it is usually possible to express the solution in terms of distributions of Green's function over a finite range, with bounded or

Received 10 November 1997; accepted for publication 3 February 1998

Q.-H. Qin, Y.-W. Mai
Dept. of Mech. & Mech. Eng., University of Sydney,
Sydney, NSW 2006, Australia

The authors wish to thank the Australian Research Council (ARC) for the continuing support of this work. Q.H. Qin is supported by an ARC Queen Elizabeth II fellowship.

integrable singular behaviour at the end points. This enables us to easily represent a crack problem with the integral equations. Recently, the simplest solution of thermoelastic Green's functions has been obtained for a two-dimensional problem of an infinite elastic plate subjected to a constant temperature discontinuity along the axis $x_2 = 0$ [9]. However, the formulation cannot be applied to the case of bimaterial problems.

In view of the above analysis, the purpose of this paper is to present the thermo-electro-elastic Green's function for bimaterial problems due to the thermal analog of a line dislocation with temperature discontinuity. The proposed Green's functions are, then, used to derive the thermoelectroelastic solution for an inclined crack near interface between two materials, which result in a system of singular integral equations. The integral equations can be solved numerically and used to calculate some fracture parameters, such as SED intensity factors and strain energy density factor.

2
Basic formulation

Consider an anisotropic piezoelectric solid in which all fields are assumed to depend only on in-plane coordinates x_1 and x_2. The SED tensor $\mathbf{\Pi}$, the elastic displacement and electric potential (EDEP) vector $\mathbf{U}$, temperature θ and heat flux $\mathbf{h} = \{h_1 h_2\}^T$ in the solid subjected to loading can be expressed in terms of complex analytic functions as follows [10,11]:

$$\begin{aligned}
\mathbf{U} &= \mathrm{Im}[\mathbf{A}\mathbf{f}(z)\mathbf{q} + \mathbf{c}g(z_t)],\\
\phi &= \mathrm{Im}[\mathbf{B}\mathbf{f}(z)\mathbf{q} + \mathbf{d}g(z_t)],\\
\mathbf{\Pi}_1 &= -\phi_{,2}, \mathbf{\Pi}_2 = \phi_{,1},\\
\theta &= \mathrm{Im}[g'(z_t)],\\
h_1 &= \mathrm{Im}[p_* ikg''(z_t)],\\
h_2 &= \mathrm{Im}[-ikg''(z_t)],
\end{aligned} \tag{1}$$

where overbars denote complex conjugation, *Im* stands for the imaginary part, $\mathbf{q}$ is a constant vector to be determined by the boundary conditions, $\mathbf{U} = \{u_1 u_2 u_3 \phi\}^T$, $\mathbf{\Pi}_j = \{\sigma_{1j}\sigma_{2j}\sigma_{3j}D_j\}^T$, $k = \sqrt{k_{11}k_{22} - k_{12}^2}$, $j = 1, 2$; $i = \sqrt{-1}$, $\mathbf{f}(z) = \{f(z_1)f(z_2)f(z_3)f(z_4)\}^T$, f and g are functions of the generalised complex variables z_i and z_t, defined by $z_i = x_1 + p_i x_2$ and $z_1 = x_1 + p_* x_2$, p_i and p_* depend on the material constants, and are determined by finding the roots of the following characteristic equations [11]:

$$\begin{aligned}
&\|\mathbf{Q} + p(\mathbf{R} + \mathbf{R}^T) + p^2\mathbf{T}\| = 0,\\
&k_{11} + 2k_{12}p_* + k_{22}p_*^2 = 0,
\end{aligned} \tag{2}$$

respectively, in which

$$\mathbf{Q}_{IK} = E_{1IK1}, \quad \mathbf{R}_{IK} = E_{1IK2}, \quad \mathbf{T}_{IK} = E_{2IK2} \ , \tag{3}$$

where k_{ij} are coefficients of heat conduction, E_{iJKm} are the generalised material constants defined by

$$E_{iJKm} = \begin{cases} C_{ijkm} & J, K = 1, 2, 3\\ e_{mij} & J = 1, 2, 3; K = 4\\ e_{ikm} & J = 4; K = 1, 2, 3\\ -\varepsilon_{im} & J = K = 4 \end{cases} \quad (i, m = 1, 2, 3) \tag{4}$$

here C_{ijkm}, e_{ijk} and ε_{jk} are elastic moduli, piezoelectric and dielectric constants, respectively.

The additional multipliers in Eq.(1) are defined by [11]

$$\begin{aligned}
&[\mathbf{Q} + p(\mathbf{R} + \mathbf{R}^T) + p^2\mathbf{T}]\mathbf{A} = 0,\\
&\mathbf{B} = \mathbf{R}^T\mathbf{A} + \mathbf{T}\mathbf{A}\mathbf{P},\\
&\mathbf{P} = \mathrm{diag}[p_1\, p_2\, p_3\, p_4],\\
&\mathbf{c} = [\mathbf{Q} + p_*(\mathbf{R} + \mathbf{R}^T) + p_*^2\mathbf{T}]^{-1}\{\boldsymbol{\beta}_1 + p_*\boldsymbol{\beta}_2\},\\
&\mathbf{d} = (\mathbf{R}^T + p_*\mathbf{T})\mathbf{c} - \boldsymbol{\beta}_2,
\end{aligned} \tag{5}$$

where

$$\boldsymbol{\beta}_1 = \{\beta_{11}\,\beta_{21}\,\beta_{31}\,\lambda_1\}^T, \boldsymbol{\beta}_2 = \{\beta_{21}\,\beta_{22}\,\beta_{32}\,\lambda_2\}^T, \tag{6}$$

in which β_{ij} and λ_i are the thermal stress coefficients and pyroelectric constants, respectively.

3
The Green's function for temperature field

3.1
Green's function for homogeneous materials

For an infinite domain subject to the thermal analog of a line dislocation with temperature discontinuity θ_0 located at $x_1 = x_2 = 0$, the solution of Eq.$(1)_4$ is of the form [9]

$$\theta(z_t) = \frac{\theta_0}{2\pi}\mathrm{Im}(\ln z_t) \ . \tag{7}$$

It is easy to show that the general solution at point z_t due to a single dislocation at $\hat{z_t} = \hat{x_1} + p_*\hat{x_2}$ is as follows:

$$\theta(z_t) = \frac{\theta_0}{2\pi}\mathrm{Im}(\ln y_1) \ . \tag{8}$$

The corresponding heat flux is given by

$$h_i = -\frac{\theta_0}{2\pi}\mathrm{Im}\left(\frac{k_{i1} + p_* k_{i2}}{y_1}\right), \tag{9}$$

where $y_1 = z_t - \hat{z_t}$.

3.2
Green's function for bimaterials

Consider a bimaterial plate for which the upper half-plane ($x_2 > 0$) is occupied by material *1*, and the lower half-plane ($x_2 < 0$) is occupied by material *2*. They are rigidly bonded together so that

$$\theta^{(1)} = \theta^{(2)}, \quad h_2^{(1)} = h_2^{(2)} \qquad \text{at } x_1 = 0, \tag{10}$$

where the superscripts (1) and (2) label the quantities relating to the material 1 and 2, respectively.

To satisfy the interface conditions Eq.(10), the solutions (8) and (9) are modified as

$$\theta^{(1)} = \frac{\theta_0}{2\pi}\mathrm{Im}(\ln y_1^{(1)}) + \frac{\theta_1}{2\pi}\mathrm{Im}(\ln y_2^{(1)}), \tag{11}$$

$$h_i^{(1)} = -\frac{\theta_0}{2\pi}\mathrm{Im}\left(\frac{k_{i1}^{(1)} + p_*^{(1)} k_{i2}^{(1)}}{y_1^{(1)}}\right) - \frac{\theta_1}{2\pi}\mathrm{Im}\left(\frac{k_{i1}^{(1)} + p_*^{(1)} k_{i2}^{(1)}}{y_2^{(1)}}\right), \tag{12}$$

for $\mathrm{Im}(z_t) > 0$, and

$$\theta^{(2)} = \frac{\theta_2}{2\pi}\mathrm{Im}(\ln y_1^{(2)}), \tag{13}$$

$$h_i^{(2)} = -\frac{\theta_2}{2\pi}\mathrm{Im}\left(\frac{k_{i1}^{(2)} + p_*^{(2)} k_{i2}^{(2)}}{y_1^{(2)}}\right), \tag{14}$$

for $\mathrm{Im}(z_t) < 0$, where θ_1 and θ_2 are two unknown constants to be determined, and $y_1^{(1)} = z_t^{(1)} - \hat{z}_t^{(1)}, y_2^{(1)} = z_t^{(1)} - \bar{\hat{z}}_t^{(1)}, y_1^{(2)} = z_t^{(2)} - \hat{z}_t^{(1)}$. It should be noted that the source point is assumed to be located in the material 1. Substitution of Eqs. (11)–(14) into Eq. (10) yields the values of θ_1 and θ_2 as

$$\theta_1 = b_1\theta_0, \quad \theta_2 = b_2\theta_0, \quad b_1 = \frac{k^{(2)} - k^{(1)}}{k^{(2)} + k^{(1)}}, \quad b_2 = \frac{2k^{(1)}}{k^{(2)} + k^{(1)}} \quad . \tag{15}$$

4
Thermoelectroelastic Green's functions

4.1
Particular solution

From Eqs. $(1)_1$, $(1)_2$ and $(1)_4$, the particular solution to the thermoelectroelastic field can be expressed as

$$\begin{aligned} \mathbf{U}_p &= \mathrm{Im}[\mathbf{c}g(z_t)], \\ \phi_p &= \mathrm{Im}[\mathbf{d}g(z_t)], \\ \theta &= \mathrm{Im}[g'(z_t)], \end{aligned} \tag{16}$$

where the subscript "p" refers to particular solution.

By comparing Eqs. (11) and (13) with Eq. $(16)_3$, the function $g(z_t)$ may be assumed in the form,

$$g^{(1)}(z_t^{(1)}) = \frac{\theta_0}{2\pi}\{y_1^{(1)}(\ln y_1^{(1)} - 1) + b_1 y_2^{(1)}(\ln y_2^{(1)} - 1)\}, \tag{17}$$

for $\mathrm{Im}(z_t^{(1)}) > 0$, and

$$g^{(2)}(z_t^{(2)}) = \frac{b_2\theta_0}{2\pi} y_1^{(2)}(\ln y_1^{(2)} - 1), \tag{18}$$

for $\mathrm{Im}(z_t^{(2)}) < 0$. The corresponding expressions for stress function and EDEP can, then, be given by

$$\begin{aligned} \mathbf{U}_p^{(1)}(z_t^{(1)}) &= \frac{\theta_0}{2\pi}\mathrm{Im}\{\mathbf{c}[y_1^{(1)}(\ln y_1^{(1)} - 1) + b_1 y_2^{(1)}(\ln y_2^{(1)} - 1)]\}, \\ \phi_p^{(1)}(z_t^{(1)}) &= \frac{\theta_0}{2\pi}\mathrm{Im}\{\mathbf{d}[y_1^{(1)}(\ln y_1^{(1)} - 1) + b_1 y_2^{(1)}(\ln y_2^{(1)} - 1)]\}, \end{aligned} \tag{19}$$

for $\mathrm{Im}(z_t^{(1)}) > 0$, and

$$\begin{aligned} \mathrm{U}_p^{(2)}(z_t^{(2)}) &= \frac{b_2\theta_0}{2\pi}\mathrm{Im}\{\mathbf{c}[y_1^{(2)}(\ln y_1^{(2)} - 1)]\}, \\ \phi_p^{(2)}(z_t^{(2)}) &= \frac{b_2\theta_0}{2\pi}\mathrm{Im}\{\mathbf{d}[y_1^{(2)}(\ln y_1^{(2)} - 1)]\}, \end{aligned} \tag{20}$$

for $\mathrm{Im}(z_t^{(2)}) < 0$. The solutions (19) and (20) do not, generally, satisfy the interface conditions at $x_2 = 0$. Therefore, a corrective solution is needed to develop when superposed on the particular solutions (19) and (20) the interface condition will be satisfied. This is completed in the coming subsection.

4.2
The thermoelectroelastic Green's functions

Again, consider a bimaterial plate for which the material *1* occupies the upper half-plane ($x_2 > 0$) and the material *2* occupies the lower half-plane ($x_2 < 0$). They are rigidly bonded so that

$$\mathbf{U}^{(1)} = \mathbf{U}^{(2)}, \quad \phi^{(1)} = \phi^{(2)} \quad \text{at } x_2 = 0 \quad . \tag{21}$$

Owing to the fact that $\mathbf{f}(\mathbf{z})$ and $g(z_t)$ have the same order to affect the EDEP and SEP in Eqs.$(1)_1$ and $(1)_2$, possible function forms come from the portion of solution $g(z_t)$. This is

$$\mathbf{f}\ (\mathbf{z}^{(i)}) = \mathrm{diag}[f(y_1^{*(i)}), f(y_2^{*(i)}), f(y_3^{*(i)}), f(y_4^{*(i)})], \quad i = 1, 2, \tag{22}$$

where

$$f(y) = y(\ln y - 1),$$
$$y_i^{*(k)} = z_i^{(k)} - \hat{z}_t^{(1)}, \quad i = 1, 2, 3, 4; k = 1, 2 \ .$$

Thus, the resulting expressions of $\mathbf{U}^{(1)}$ and $\phi^{(1)}$ can be given as

$$\mathrm{U}^{(1)} = \mathrm{Im}[\mathbf{A}^{(1)}\mathbf{f}(\mathbf{z}^{(1)})\mathbf{q}_1] + \frac{\theta_0}{2\pi}\mathrm{Im}\{\mathbf{c}^{(1)}[y_1^{(1)}(\ln y_1^{(1)} - 1) + b_1 y_2^{(1)}(\ln y_2^{(1)} - 1)]\}, \tag{23}$$

$$\phi^{(1)} = \mathrm{Im}[\mathbf{B}^{(1)}\mathbf{f}(\mathbf{z}^{(1)})\mathbf{q}_1] + \frac{\theta_0}{2\pi}\mathrm{Im}\{\mathbf{d}^{(1)}[y_1^{(1)}(\ln y_1^{(1)} - 1) + b_1 y_2^{(1)}(\ln y_2^{(1)} - 1)]\}, \tag{24}$$

for $\mathrm{Im}(z_t^{(1)}) > 0$, and

$$\mathbf{U}^{(2)} = \mathrm{Im}[\mathbf{A}^{(2)}\mathbf{f}(\mathbf{z}^{(2)})\mathbf{q}_2] + \frac{b_2\theta_0}{2\pi}\mathrm{Im}\{\mathbf{c}^{(2)}y_1^{(2)}(\ln y_1^{(2)} - 1)\}, \tag{25}$$

$$\phi^{(2)} = \mathrm{Im}[\mathbf{B}^{(2)}\mathbf{f}(\mathbf{z}^{(2)})\mathbf{q}_2] + \frac{b_2\theta_0}{2\pi}\mathrm{Im}\{\mathbf{d}^{(2)}y_1^{(2)}(\ln y_1^{(2)} - 1)\}, \tag{26}$$

for $\mathrm{Im}(z_t^{(2)}) < 0$ The substitution of Eqs. (23)–(26) into Eq. (21) yields

$$\begin{aligned}
\mathbf{A}^{(1)}\mathbf{q}_1 - \mathbf{A}^{(2)}\mathbf{q}_2 &= \frac{\theta_0}{2\pi}[b_2\mathbf{c}^{(2)} + b_1\overline{\mathbf{c}}^{(1)} - \mathbf{c}^{(1)}] \ , \\
\mathbf{B}^{(1)}\mathbf{q}_1 - \mathbf{B}^{(2)}\mathbf{q}_2 &= \frac{\theta_0}{2\pi}[b_2\mathbf{d}^{(2)} + b_1\overline{\mathbf{d}}^{(1)} - \mathbf{d}^{(1)}] \ .
\end{aligned} \tag{27}$$

Solving Eq.(27) for $\mathbf{q}_1$ and $\mathbf{q}_2$, one obtains

$$\begin{aligned}
\mathbf{q}_1 &= \frac{\theta_0}{2\pi}[\mathbf{B}^{(1)} - \mathbf{B}^{(2)}\mathbf{A}^{(2)-1}\mathbf{A}^{(1)}]^{-1} \\
&\quad \times \{[b_2\mathbf{d}^{(2)} + b_1\overline{\mathbf{d}}^{(1)} - \mathbf{d}^{(1)}] - \mathbf{B}^{(2)}\mathbf{A}^{(2)-1}[b_2\mathbf{c}^{(2)} + b_1\overline{\mathbf{c}}^{(1)} - \mathbf{c}^{(1)}]\}, \\
\mathbf{q}_2 &= \frac{\theta_0}{2\pi}[\mathbf{B}^{(1)}\mathbf{A}^{(1)-1}\mathbf{A}^{(2)} - \mathbf{B}^{(2)}]^{-1} \\
&\quad \times \{[b_2\mathbf{d}^{(2)} + b_1\overline{\mathbf{d}}^{(1)} - \mathbf{d}^{(1)}] - \mathbf{B}^{(1)}\mathbf{A}^{(1)-1}[b_2\mathbf{c}^{(2)} + b_1\overline{\mathbf{c}}^{(1)} - \mathbf{c}^{(1)}]\}
\end{aligned} \tag{28}$$

Thus, the thermoelectroelastic Green's functions can be obtained by substituting Eq. (28) into Eqs. (23)–(26).

Now, let us discuss the image singularities properties of Eqs. (23)–(26). The first term in Eq. (23) represents image singularities for material *1* which are located at the upper half-plane occupied by the material. They can be shown by writing

$$y_j^{*(1)} = z_j^{(1)} - \hat{z}_t^{(1)} = z_j^{(1)} - z_j^{t(1)}, \tag{29}$$

with

$$\begin{aligned}
z_j^{t(1)} &= x_{j1}^{t(1)} + p_j^{(1)}x_{j2}^{t(1)} = \hat{x}_1 + p_*^{(1)}\hat{x}_2 \ , \\
p_j^{(1)} &= p_{jR}^{(1)} + ip_{j1}^{(1)}, \ p_*^{(1)} = \frac{1}{k_{22}^{(1)}}(k_{12}^{(1)} + i\sqrt{k_{11}^{(1)}k_{22}^{(1)} - (k_{12}^{(1)})^2}) \ .
\end{aligned} \tag{30}$$

The last equality in Eq.$(30)_1$ provides the equations to determine locations of the image singularity as

$$x_{j1}^{t(1)} + p_{jR}^{(1)} x_{j2}^{t(1)} = \hat{x}_1 + \frac{k_{12}^{(1)} \hat{x}_2}{k_{22}^{(1)}}, \quad p_{j1}^{(1)} x_{(j2)}^{t(1)} = \frac{\hat{x}_2}{k_{22}^{(1)}} \sqrt{k_{11}^{(1)} k_{22}^{(1)} - (k_{12}^{(1)})^2} \ . \tag{31}$$

Since $p_{j1}^{(1)}$ and $\hat{x}_2$ are positive by definition, it follows that $x_{j2}^{t(1)} > 0$, which indicates that the image singularity for $f(y_{j1}^{*(1)})$ is located in the upper half-plane. The image singularities for Eq.(25) can be obtained similarly, and they are also located in the material *1*. The conclusion is that there are five image singularities, four of which are located in the upper half-plane, and the other one image singularity is in the lower half-plane.

5
Interaction between crack and interface

5.1
Boundary conditions

The geometrical configuration of the problem to be solved is depicted in Fig. 1, showing a crack with an orientation angle α and length *2c* near an interface between materials *1* and *2*. The corresponding boundary conditions are as follows:

– *along the inclined crack*

$$\begin{aligned} \mathbf{t}_n &= -\mathbf{\Pi}_1 \sin\alpha + \mathbf{\Pi}_2 \cos\alpha = 0, \\ h_n &= -h_1 \sin\alpha + h_2 \cos\alpha = 0, \end{aligned} \tag{32}$$

– *at infinity*

$$h_2^{\infty} = h_0, \quad \mathbf{\Pi}_1^{\infty} = \mathbf{\Pi}_2^{\infty} = h_1^{\infty} = 0, \tag{33}$$

where *n* stands for the normal direction to the lower face of the inclined crack, $\mathbf{t}_n$ is the surface traction-charge vector.

It is convenient to represent the solution as the sum of a uniform heat flux in an unflawed solid which involves no thermal stress and a corrective solution in which the boundary conditions are:

– *along the inclined crack*

$$\begin{aligned} \mathbf{t}_n &= -\mathbf{\Pi}_1 \sin\alpha + \mathbf{\Pi}_2 \cos\alpha = 0, \\ h_n &= -h_1 \sin\alpha + h_2 \cos\alpha = -h_0 \cos\alpha, \end{aligned} \tag{34}$$

– *at infinity*

$$\mathbf{\Pi}_1^{\infty} = \mathbf{\Pi}_2^{\infty} = h_1^{\infty} = h_2^{\infty} = 0 \ . \tag{35}$$

In the following sections, we will use Eqs. (34) and (35) instead of Eqs.(32) and (33).

5.2
Singular integral equations

The boundary conditions $(34)_2$, can be satisfied by redefining the discrete Green's functions θ_0 in Eq.(12) in terms of distributing Green's functions $\theta_0(\xi)$ defined along the crack line

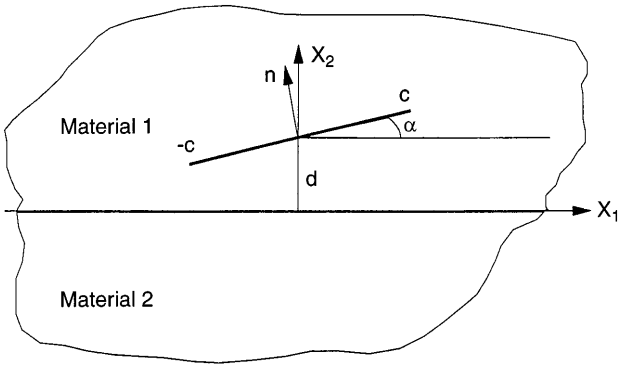

Fig. 1. Geometry of the inclined crack

$$z_t^{(1)} = p_*^{(1)} d + \eta z^*,\ \hat{z}_t^{(1)} = p_*^{(1)} d + \xi z^*,\ z^* = \cos\alpha + p_*^{(1)} \sin\alpha,$$

where d and α are shown in Fig. 1. Enforcing the satisfaction of the applied heat flux conditions on the crack faces, a singular integral equation for the Green's function is obtained as

$$\frac{1}{\pi}\mathrm{Re}\left[\int_{-1}^{1}\left[\frac{1}{t_0 - t} + K_0(t_0, t)\right]\hat{\theta}_0(t)\mathrm{d}t\right] = \frac{2h_0\cos\alpha}{k^{(1)}}, \tag{36}$$

where

$$\hat{\theta}_0(t) = \theta_0(\xi), t = c\xi, t_0 = c\eta,$$

and

$$K_0(t_0, t) = b_1\mathrm{Im}\left[\frac{z^*}{ct_0 z^* - ct\overline{z}^* + (p_*^{(1)} - \overline{p}_*^{(1)})d}\right], \tag{37}$$

is a regular function.

In addition to Eq.(36), the single-valuedness of the temperature around a closed contour surrounding the whole crack requires that

$$\int_{-1}^{1}\hat{\theta}_0(t)\mathrm{d}t = 0. \tag{38}$$

The singular integral equation (36), combined with Eq.(38), can be solved numerically [12]. To this end, let

$$\hat{\theta}_0(t) = \frac{\Theta(t)}{\sqrt{1 - t^2}} \approx \frac{\sum_{k=1}^{n} B_k T_k(t)}{\sqrt{1 - t^2}}, \tag{39}$$

where $\Theta(t)$ is a regular function defined in a closed interval $|t| \le 1$, B_k are the real unknown coefficients, and $T_k(t)$ the Chebyshev polynomials. Thus, the discretized form of Eqs.(36) and (38) may be written as [12]

$$\begin{aligned}
&\sum_{k=1}^{n}\frac{\Theta(t_k)}{n}\left[\frac{1}{t_{0r} - t_k} + K_0(t_{0r}, t_k)\right] = \frac{2h_0\cos\alpha}{k^{(1)}},\\
&\sum_{k=1}^{n}\Theta(t_k) = 0,
\end{aligned} \tag{40}$$

where

$$t_k = \cos\left[\frac{(2k-1)\pi}{2n}\right],\quad k = 1, 2, \ldots, n,$$

$$t_{0r} = \cos\left(\frac{r\pi}{n}\right),\quad r = 1, 2, \ldots, n-1.$$

Equation (40) provides a system of n linear algebraic equation to determine $\Theta(t_k)$, and then B_k. Once the function $\Theta(t)$ has been found, the corresponding SED can be given from Eqs.$(1)_3$ and (24) in the form

$$\begin{aligned}
\mathbf{\Pi}_1^{(1)} &= -\boldsymbol{\phi}_{,2}^{(1)} = -\frac{1}{2\pi}\int_{-c}^{c}\mathrm{Im}[\mathbf{B}^{(1)}\mathbf{P}^{(1)}\langle\ln\mathbf{z}^{(1)}\rangle\mathbf{q}_1 + \mathbf{d}^{(1)}p_*^{(1)}(\ln y_1^{(1)} + b_1\ln y_2^{(1)}]\theta_0(\xi)\mathrm{d}\xi,\\
\mathbf{\Pi}_2^{(1)} &= \boldsymbol{\phi}_{,1}^{(1)} = \frac{1}{2\pi}\int_{-c}^{c}\mathrm{Im}[\mathbf{B}^{(1)}\langle\ln\mathbf{z}^{(1)}\rangle\mathbf{q}_1 + \mathbf{d}^{(1)}(\ln y_1^{(1)} + b_1\ln y_2^{(1)}]\theta_0(\xi)\mathrm{d}\xi,
\end{aligned} \tag{41}$$

where

$$\langle \ln \mathbf{z}^{(1)} \rangle = \mathrm{diag}[\ln y_1^{*(1)}, \ln y_2^{*(1)}, \ln y_3^{*(1)}, \ln y_4^{*(1)}],$$
$$y_i^{*(1)} = z_i^{(1)} - \hat{z}_i^{(1)} = z_i^{(1)} - \xi z^* - p_*^{(1)} d, \qquad i = 1, 2, 3, 4. \tag{42}$$

Thus, the traction-charge vector on the crack faces is of the form

$$\begin{aligned}\mathbf{t}_n(\eta) &= -\mathbf{\Pi}_1^{(1)}(\eta) \sin\alpha + \mathbf{\Pi}_2^{(1)}(\eta) \cos\alpha \\ &= \frac{1}{2\pi} \int_{-c}^{c} \mathrm{Im}\,[\mathbf{B}^{(1)}(\mathbf{I}\cos\alpha + \mathbf{P}^{(1)} \sin\alpha)\langle \ln \mathbf{z}^{(1)} \rangle \mathbf{q}_1 \\ &\qquad + \mathbf{d}^{(1)}(\cos\alpha + p_*^{(1)} \sin\alpha)(\ln y_1^{(1)} + b_1 \ln y_2^{(1)})]\theta_0(\xi)\mathrm{d}\xi. \end{aligned} \tag{43}$$

It is obvious that $\mathbf{t}_n(\eta) \neq 0$ on the crack faces $|\eta| \leq c$. To satisfy the traction-charge-free condition $(34)_1$, we must superpose a solution of the corresponding isothermal problem with a traction-charge vector equal and opposite to that of Eq.(43) in the range $|\eta| \leq c$. The elastic solution for a singular dislocation of strength $\mathbf{b}_0$ has been given in the literature [10]. This solution can be straightforwardly extended to the case of electroelastic problem as

$$\begin{aligned}\mathbf{\Pi}_1^{(1)} &= -\frac{1}{\pi} \mathrm{Im}[\mathbf{B}^{(1)} \langle p_i^{(1)} (z_i^{(1)} - p_i^{(1)} d)^{-1} \rangle \mathbf{B}^{(1)T}] \mathbf{b}_0 \\ &\quad - \frac{1}{\pi} \sum_{\beta=1}^{4} \mathrm{Im}[\mathbf{B}^{(1)} \langle p_i^{(1)} (z_i^{(1)} - \overline{p}_\beta^{(1)} d)^{-1} \rangle \mathbf{B}^* \mathbf{I}_\beta \overline{\mathbf{B}}^{(1)T}] \mathbf{b}_0 \end{aligned} \tag{44}$$

$$\begin{aligned}\mathbf{\Pi}_2^{(1)} &= \frac{1}{\pi} \mathrm{Im}[\mathbf{B}^{(1)} \langle (z_i^{(1)} - p_i^{(1)} d)^{-1} \rangle \mathbf{B}^{(1)T}] \mathbf{b}_0 \\ &\quad + \frac{1}{\pi} \sum_{\beta=1}^{4} \mathrm{Im}[\mathbf{B}^{(1)} \langle (z_i^{(1)} - \overline{p}_\beta^{(1)} d)^{-1} \rangle \mathbf{B}^* \mathbf{I}_\beta \overline{\mathbf{B}}^{(1)T}] \mathbf{b}_0 \end{aligned} \tag{45}$$

where
$\mathbf{I}_\beta = \mathrm{diag}[\delta_{1\beta}\delta_{2\beta}\delta_{3\beta}\delta_{4\beta}], \delta_{ij} = 1 \quad \text{for} i = j,$
$\delta_{ij} = 0$ for $i \neq j$, and
$\langle ()_i \rangle = \mathrm{diag}[()_1 ()_2 ()_3 ()_4],$
$\mathbf{B}^* = \mathbf{B}^{(1)-1}[\mathbf{I} - \mathbf{2}(\mathbf{M_1^{-1}} + \overline{\mathbf{M}}_\mathbf{2}^{-\mathbf{1}})^{-\mathbf{1}} \mathbf{L}^{-\mathbf{1}}]$

with

$$\mathbf{M}_j = -i\mathbf{B}^{(j)} \mathbf{A}^{(j)-1}, \qquad j = 1, 2,$$
$$\mathbf{L} = -2i\mathbf{B}^{(1)} \mathbf{B}^{(1)T}.$$

Therefore, the boundary condition $(34)_1$ will be satisfied if

$$\frac{\mathbf{L}}{2\pi} \int_{-c}^{c} \frac{\mathbf{b}_0(\xi)\mathrm{d}\xi}{\eta - \xi} + \int_{-c}^{c} \mathbf{K}_0(\eta, \xi) \mathbf{b}_0(\xi)\mathrm{d}\xi = -\mathbf{t}_n(\eta), \tag{46}$$

where

$$\mathbf{K}_0(\eta, \xi) = \frac{1}{\pi} \sum_{\beta=1}^{4} \mathrm{Im}[\mathbf{B}^{(1)} \langle z_j^* (z_j^{(1)} - \hat{z}_{\beta c}^{(1)})^{-1} \rangle \mathbf{B}^* \mathbf{I}_\beta \overline{\mathbf{B}}^{(1)T} \quad , \tag{47}$$

with

$$z_j^* = \cos\alpha + p_j^{(1)} \sin\alpha, \quad z_j^{(1)} = \eta z_j^* + p_j^{(1)} d, \quad \hat{z}_{\beta c}^{(1)} = \xi z_\beta^* + p_\beta^{(1)} d.$$

For single-valued displacements and electric potential around a closed contour surrounding the whole crack, the following conditions have also to be satisfied:

$$\int_{-c}^{c} \mathbf{b}_0(\xi)\mathrm{d}\xi = 0. \tag{48}$$

As was done previously, let $\eta = ct_0$, $\xi = ct$, and

$$\mathbf{b}_0(\xi) = \frac{\boldsymbol{\Theta}(\xi)}{\sqrt{c^2 - \xi^2}} \approx \frac{\sum_{k=1}^{n} \mathbf{E}_k T_k(t)}{\sqrt{1 - t^2}}, \tag{49}$$

where $\mathbf{E}_k = \{E_{k1}, E_{k2}, E_{k3}, E_{k4}\}^T$. Thus, from Eqs.(46) and (48), we obtain

$$\begin{aligned} &\sum_{k=1}^{m} \frac{1}{n}\left[\frac{\mathbf{L}}{2c(t_{0r} - t_k)} + \mathbf{K}_0(t_{0r}, t_k)\right]\boldsymbol{\Theta}(ct_k) = -\mathbf{t}_n(t_{0r}), \\ &\sum_{k=1}^{m} \boldsymbol{\Theta}(ct_k) = 0. \end{aligned} \tag{50}$$

Equations (50) provide a system of $4m$ linear algebraic equations to determine $\boldsymbol{\Theta}(ct_k)$ and then $\mathbf{E}_k$. Once the function $\boldsymbol{\Theta}(ct_k)$ has been found from Eq.(50), the stresses and electric displacements $\boldsymbol{\Pi}_n(\eta)$ in a coordinate local to the crack line can be expressed in the form

$$\boldsymbol{\Pi}_n(\eta) = \boldsymbol{\Omega}(\alpha)\left\{\frac{\mathbf{L}}{2\pi}\int_{-c}^{c} \frac{\mathbf{b}_0(\xi)\mathrm{d}\xi}{\eta - \xi} + \int_{-c}^{c} \mathbf{K}_0(\eta, \xi)\mathbf{b}_0(\xi)\mathrm{d}\xi + \mathbf{t}_n(\eta)\right\}, \tag{51}$$

where the 4×4 matrix $\boldsymbol{\Omega}(\alpha)$, whose components are the cosine of the angle between the local coordinates and the global coordinates, is in the form

$$\boldsymbol{\Omega}(\alpha) = \begin{bmatrix} \cos\alpha & \sin\alpha & 0 & 0 \\ -\sin\alpha & \cos\alpha & 0 & 0 \\ 0 & 0 & 1 & 0 \\ 0 & 0 & 0 & 1 \end{bmatrix}. \tag{52}$$

Using Eq.(31), we can evaluate the stress-intensity factors

$$\mathbf{K}^* = \{K_{\mathrm{II}}, K_{\mathrm{I}}, K_{\mathrm{III}}, K_{\mathrm{D}}\}^T$$

at the tips, e.g. at the right tip of the crack ($\xi = c$) by the following definition:

$$\mathbf{K}^* = \lim_{\xi \to c^+} \sqrt{2\pi(\xi - c)}\boldsymbol{\Pi}_n(\xi). \tag{53}$$

Combined with the results of Eq.(31), it then leads to

$$\mathbf{K}^* \approx \sqrt{\frac{\pi}{4c}}\boldsymbol{\Omega}(\alpha)\mathbf{L}\boldsymbol{\Theta}(c). \tag{54}$$

Thus, the solution of the singular integral equation enables the direct determination of the stress-intensity factors.

5.3
Direction of crack initiation

The strain energy density criterion [13] will be used to predict the direction of crack initiation in the thermopiezoelectric bimaterials. To make the derivation tractable, the crack tip fields are first studied. In doing this, a polar coordinate system (r, ω) centred at a crack tip, say the right tip of the crack, $(x_1, x_2) = (c\cos\alpha, d + c\sin\alpha)$ and $\omega = 0$ along the crack line is used, Then, the variable $z_k^{(1)}$ becomes

$$z_k^{(1)} = p_k^{(1)} d + c(\cos\alpha + p_k^{(1)} \sin\alpha) + r[\cos(\alpha+\omega) + p_k^{(1)} \sin(\alpha+\omega)]. \tag{55}$$

With this coordinate system, SED fields near the crack tip can be evaluated by taking the asymptotic limit of Eq.(51), and using expressions (44) and (45) as $r \to 0$

$$\mathbf{\Pi}_1^{(1)}(r,\omega) \approx \sqrt{\frac{1}{2cr}}\mathrm{Im}[\mathbf{B}^{(1)}\left\langle \frac{p_k^{(1)}}{\sqrt{z_k^*(\alpha) z_k^*(\alpha+\omega)}} \right\rangle \mathbf{B}^{(1)T}]\mathbf{\Theta}(c) = \sqrt{\frac{1}{2cr}}\mathbf{V}_1(\omega), \tag{56}$$

$$\mathbf{\Pi}_2^{(1)}(r,\omega) \approx -\sqrt{\frac{1}{2cr}}\mathrm{Im}[\mathbf{B}^{(1)}\left\langle \frac{1}{\sqrt{z_k^*(\alpha) z_k^*(\alpha+\omega)}} \right\rangle \mathbf{B}^{(1)T}]\mathbf{\Theta}(c) = \sqrt{\frac{1}{2cr}}\mathbf{V}_2(\omega), \tag{57}$$

where

$$z_k^*(x) = \cos x + p_k^{(1)} \sin x$$

For a thermopiezoelectric material, the strain energy density factor $S(\omega)$ can be calculated by considering the related thermoelectroelastic potential energy W. The relationship between the two functions is as follows:

$$S(\omega) = rW = \frac{r}{2}\{\mathbf{\Pi}_1\mathbf{\Pi}_2\}^T \mathbf{F} \{\mathbf{\Pi}_1\mathbf{\Pi}_2\}, \tag{58}$$

where the matrix **F** is the inverse of stiffness matrix **E**. The substitution of Eqs.(56) and (57) into Eq.(58), leads to

$$S(\omega) = \frac{1}{4c}\{\mathbf{V}_1\mathbf{V}_2\}^T \mathbf{F} \{\mathbf{V}_1\mathbf{V}_2\}. \tag{59}$$

Referring to the Ref. [14], the strain energy density criterion states that the direction of crack initiation coincides with the direction of the strain energy density factor S_{min}, i.e. the necessary and sufficient condition of crack growth in the direction ω_0 is that

$$\left.\frac{\partial S}{\partial \omega}\right|_{\omega=\omega_0} = 0 \text{ and } \left.\frac{\partial^2 S}{\partial \omega^2}\right|_{\omega=\omega_0} > 0. \tag{60}$$

Substituting Eq.(59) into Eq.$(60)_1$, yields

$$\{\mathbf{V}_{1i}\mathbf{V}_{2i}\}^T \mathbf{F} \frac{\partial}{\partial \omega}\{\mathbf{V}_{1i}\mathbf{V}_{2i}\}^T = 0. \tag{61}$$

Solving Eq.(61) several roots of ω may be obtained. The fracture angle ω_0 will be the one satisfying Eq.$(60)_2$.

6 Numerical results

In this section, the numerical results for fracture angle are presented to illustrate the applications of the proposed formulation. For simplicity, we only consider an inclined crack near the interface between two transversely isotropic materials. The upper and lower materials are assumed to be $BaTiO_3$ [15] and cadmium selenide [16], respectively. The material constants for the two materials are as follows:

(1) material properties for $BaTiO_3$ [15]

$$\begin{aligned}
&c_{11} = 150\text{GPa}, c_{12} = 66\text{GPa}, c_{13} = 66\text{GPa}, c_{33} = 146\text{GPa}, c_{44} = 44\text{GPa},\\
&\alpha_{11} = 8.53 \times 10^{-6}/\text{K}, \alpha_{33} = 1.99 \times 10^{-6}/\text{K}, \lambda_3 = 0.133 \times 10^5 \text{N/CK},\\
&e_{31} = -4.35\text{C/m}^2, e_{33} = 17.5\text{C/m}^2, e_{15} = 11.4\text{C/m}^2, \kappa_{11} = 1115\kappa_0,\\
&\kappa_{33} = 1260\kappa_0, \kappa_0 = 8.85 \times 10^{-12}\text{C}^2/\text{Nm}^2,
\end{aligned}$$

(2) material properties of cadmium selenide [16]

$$c_{11} = 74.1\text{GPa}, c_{12} = 45.2\text{GPa}, c_{13} = 39.3\text{GPa}, c_{33} = 83.6\text{GPa}, c_{44} = 13.2\text{GPa},$$

$$\gamma_{11} = 0.621 \times 10^6 \text{NK}^{-1}\text{m}^{-2}, \gamma_{33} = 0.551 \times 10^6 \text{NK}^{-1}\text{m}^{-2}, \chi_3 = -0.294\text{CK}^{-1}\text{m}^{-2},$$

$$e_{31} = -0.160\text{Cm}^{-2}, e_{33} = 0.347\text{Cm}^{-2}, e_{15} = 0.138\text{Cm}^{-2},$$

$$\kappa_{11} = 82.6 \times 10^{-12}\text{C}^2/\text{Nm}^2, \kappa_{33} = 90.3 \times 10^{-12}\text{C}^2/\text{Nm}^2,$$

in which the well-known two-index notation has been adopted [17]. Here, c_{ij} and e_{ij} are the reduced material constants obtained by using the following convention: replace ij or kl by p or q, where i, j, k, l take the values of 1–3, and p, q assume the values 1–6 according to the following rule:

ij or kl	11	22	33	23 or 32	31 or 13	12 or 21
p or q	1	2	3	4	5	6

In accordance to this representation, it follows that

$$c_{pq} = C_{ijkl}, e_{ip} = e_{ikl}, \text{ for } i, j, k, l = 1\text{–}3, p, q = 1\text{–}6.$$

Since the values of the coefficient of heat conduction both for $BaTiO_3$ and cadmium selenide could not be found in the literature, the values $k_{33}^{(1)}/k_{11}^{(1)} = 1.5, k_{33}^{(2)}/k_{11}^{(2)} = 2$, and $k_{13}^{(1)} = k_{13}^{(2)} = 0$ are assumed.

Figure 2 shows the variation of the fracture angle ω_0 with the crack orientation α. It is found from the figure that the fracture angle ω_0 varies between -57° and -35°, and reaches its minimum value at about $\alpha = 37^\circ$.

7 Conclusion

The thermoelectroelastic Green's functions for bimaterials due to a thermal analog of line dislocation with temperature discontinuity are developed using the Stroh formalism. The study shows that the Green's function for bimaterials due to a temperature discontinuity in the upper half plane has four image singularities located in the upper half-plane, and another image singularity located in the lower half-plane. Based on the proposed thermoelectroelastic Green's functions, a system of singular integral equations is derived to model fracture problems of a crack near a bimaterial interface between dissimilar thermopiezoelectric materials. The formulations can be used to calculate some fracture parameters, such as SED intensity factors and strain energy density factor. As a result, the direction of crack growth can be predicted by way of the strain energy density theory. Numerical results for crack growth direction at a particular crack tip of the crack system are presented to illustrate the application of the proposed formulation.

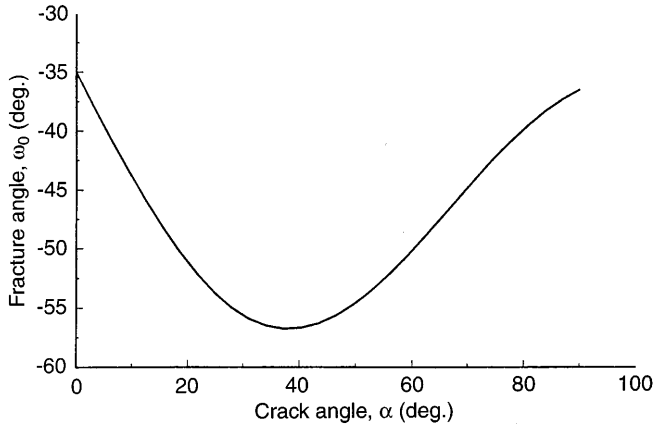

Fig. 2. Fracture angle vs crack orientation

References

1. **Olesiak, Z.; Sneddon, I. N.:** The distribution of thermal stress in an infinite elastic solid containing a penny-shaped crack. Arch. Rational Mech. Anal. 4 (1960) 238–254
2. **Sih, G. C:** On the singular character of thermal stresses near a crack tip. J. Appl. Mech. 29 (1962) 587–589
3. **Florence, A. L.; Goodier, J. N.:** The linear thermoelastic problem of uniform heat flow disturbed by a penny-shaped insulated crack. Int. J. Eng. Sci. 1 (1963) 533–540
4. **Clements, D. L.:** Thermal stress in an anisotropic elastic half-space. SIAM J. Appl. Math. 24 (1973) 332–337
5. **Atkinson, C.; Clements, D. L.:** On some crack problems in anisotropic thermoelasticity. Int. J. Solids Struct. 13 (1977) 855–864
6. **Tsai, Y. M.:** Transversely isotropic thermoelastic problem of uniform heat flow disturbed by a penny-shaped crack. J. Thermal Stresses 6 (1983) 379–389
7. **Hwu, C.:** Thermal stresses in an anisotropic plate disturbed by an insulated elliptic hole or crack. J. Appl. Mech. 57 (1990) 916–922
8. **Dunders, J.; Comninou, M.:** Green's function for planar thermoelastic contact problems-Exterior contact. Mech. Res. Commun. 6 (1979) 309–316
9. **Sturla, F. A.; Barber, J. R.:** Thermal stresses due to a plane crack in general anisotropic material. J. Appl. Mech. 55 (1988) 372–376
10. **Ting, T. C. T.:** Image singularities of Green's functions for anisotropic elastic half-space and bimaterials. Quart. J. Mech. Appl. Math. 45 (1992) 119–139
11. **Yu, S. W.; Qin, Q.H.:** Damage analysis of thermopiezoelectric properties: Part I-crack tip singularities. Theore. Appl. Fracture Mech. 25 (1996) 263–277
12. **Erdogan, F.; Gupta, G. D.:** On the numerical solution of singular integral equations. Quart. Appl. Math. 32 (1972) 525–534
13. **Sih, G. C.:** A special theory of crack propagation, methods of analysis and solutions of crack problems. In: Sih, G. C. (ed.) Mechanics of fracture I, pp. 21–45. Leiden: Noordhoff International Publishing 1973
14. **Sih, G. C.:** Prediction of crack growth under mixed mode conditions. In: Sih, G.C.; Theocaris, P.S. (eds.): USA-Greece symposium on mixed mode crack propagation, pp. 3–19. The Netherlands: Sijthoff & Noordhoff 1981
15. **Dunn, M. L.:** Micromechanics of coupled electroelastic composites: effective thermal expansion and pyroelectric coefficients. J. Appl. Phys. 73 (1993) 5131–5140
16. **Ashida, F.; Tauchert, Th. R.; Noda, N.:** A general solution technique for piezothermoelasticity of hexagonal solids of class 6mm in Certesian coordinates. Z. Angew. Math. Mech. 74 (1994) 87–95
17. **Nye, J. F.:** Physical properties of crystals. Oxford: Oxford University Press 1957